Selected Paper

Preparation and Characterization of LiCl-Occluded LiLSX Zeolite

Satoshi Yoshida,* Atsushi Harada, Kunikazu Kamioka,[1] and Masao Nakano

Nanyo Research Laboratory, TOSOH Corporation, Shunan, Yamaguchi 746-8501

[1]TOSOH Analysis and Research Center, Shunan, Yamaguchi 746-0006

Received May 19, 2003; E-mail: s_yosi@tosoh.co.jp

LiCl-occluded LiLSX (Li exchanged Low Silica X zeolite with Si/Al = 1.0) was prepared by a heat treatment after evaporating a LiLSX or NaLSX slurry with LiCl, followed by lithium exchange in the case of NaLSX. The amount of occluded LiCl increased with increasing of the temperature. LiCl-occluded LiLSX prepared from NaLSX had a higher crystallinity than that prepared from LiLSX. The difference in crystallinity is explained as being related to the difference in the distortion of the skeleton structure of the zeolites. Chloride anions in high-crystallinity LiCl-occluded LiLSX were found to be located in sodalite cages by a Fourier synthesis of the powder X-ray diffraction pattern. The location of lithium cations was investigated based on the adsorption properties of nitrogen at room temperature and existing data on salt-occluded zeolites. Lithium cations in LiCl-occluded LiLSX are thought to simultaneously occupy the adjacent sites I and I′.

The occlusion of salts in the zeolite framework has been studied for many years.[1–4] Salt-occluded zeolites are categorized into two groups according to whether the occlusion is reversible or irreversible.[3] In the former case, the salt would be located in large cavities such as supercages in X or Y zeolite, and can be readily washed out, whereas, in the latter case, the salt is located in small cavities such as the sodalite cages in X or Y zeolite, and cannot be washed out. Irreversibly salt-occluded zeolite is prepared by either a molten salt treatment at high temperature or a heat treatment following evaporation of the zeolite slurry containing the salt solution.

Various aspects of salt-occluded zeolites have been investigated, such as their preparation[1–5] and characterization;[1–4,6–14] for industrial applications, modifications of the catalysis[2] and the occlusion of ungreen salt like eutectic LiCl–KCl from spent nuclear fuel.[15,16] As for types of zeolites, there have been many reports on sodalite[3,4,6–11] and Y zeolite.[2–5,12,13] However, little has been reported on salt-occluded X zeolite,[1,3,4,14] and no reports exist on LSX zeolite having the maximum number of cations per unit cell with the same FAU structure as X and Y zeolite.

This work focused on the preparation and characterization of salt-occluded LSX. Lithium ions were chosen as charge compensation cations in an attempt to modify the room-temperature nitrogen and oxygen adsorption properties of LiLSX, which is the best adsorbent for oxygen pressure swing adsorption in industrial use at present.[17]

The effect of varying the heat-treatment temperature and the ionic type of the starting zeolites during the preparation of irreversibly LiCl-occluded LiLSX (*ir*-LiCl/LiLSX) was investigated. *ir*-LiCl/LiLSX was characterized by powder X-ray diffraction (XRD) and its Fourier synthesis. The nitrogen and oxygen adsorption capacities of *ir*-LiCl/LiLSX at room temperature were measured and compared with those of LiLSX and reversibly LiCl-occluded LiLSX (*re*-LiCl/LiLSX). The locations of Li cations were deduced from the adsorption properties and existing data on salt-occluded zeolites.

Experimental

Preparation. The *ir*-LiCl/LiLSX was prepared by a modified version of Rabo et al.'s method.[2] The process is shown in Fig. 1. Zeolite NaKLSX with Si/Al = 1.00 was synthesized by Kuhl's method.[18] 100% Li-exchanged LSX (LiLSX) and 100% Na-exchanged LSX (NaLSX), which are the starting materials for the reaction of zeolite and LiCl, were prepared by conventional ion-exchange reactions from NaKLSX using a chloride solution (pH = 11; adjusted by LiOH or NaOH).

The starting zeolites, LiLSX or NaLSX, were slurried with a solution of LiCl (pH = 11; adjusted by LiOH). The LiCl content was a 6-fold excess of Cl per sodalite cage of LSX, because preliminary experiments revealed that the occlusion reaction proceeded more

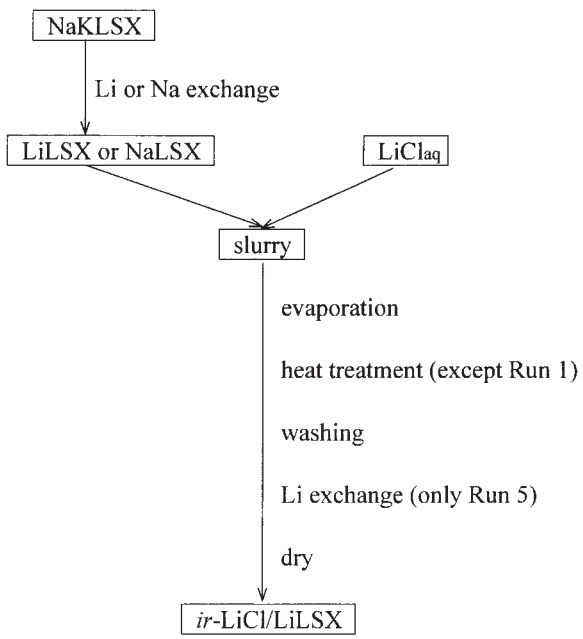

Fig. 1. Preparation flow of *ir*-LiCl/LiLSX.

Published on the web February 10, 2004; DOI 10.1246/bcsj.77.387

rapidly with excess LiCl. The slurries were evaporated in a rotary evaporator at 333 K. The zeolites with highly dispersed LiCl were pelletized without any binder, and sieved into a fraction of approximately 0.5–2.0 mm diameter. The pellets, placed into the back end of a tube furnace with a pre-heat zone under nitrogen flow to prevent zeolite crystals from collapsing due to water vapor at high temperatures, were heated at a fixed temperature for 3 h.

The reactants were washed by a dilute LiOH solution (pH = 11), which was used to prevent hydrolysis, until the filtrate of the wash proved negative to a chloride ion test with $AgNO_3$. When the starting zeolite was NaLSX, the reactant was further exchanged by lithium by a conventional method using a LiCl solution (pH = 11; adjusted by LiOH).

For a comparison of the nitrogen adsorption characteristics, a *re*-LiCl/LiLSX with Li/Al = 1.08 was also prepared. LiLSX slurried with a solution of LiCl (pH = 11; adjusted by LiOH) was evaporated at 333 K and treated without heat except for dehydration at 623 K performed for a nitrogen adsorption measurement. The reversibility of LiCl was determined by the ratio of lithium to aluminum after washing with a dilute LiOH solution (pH = 11).

Characterization. The occluded LiCl amounts were assessed by the excess level of cations per aluminum, as determined by an inductively coupled plasma–atomic emission spectroscope (Perkin Elmer, Optima 3000). The crystallinities of *ir*-LiCl/LiLSX were estimated by powder XRD; hydrated samples with 80% relative humidity at 298 K were measured by a Philips, PW1700. The crystallinities were approximated by the relative intensity areas of the sum of the three peaks at 533, 642, 555, compared with LiLSX.

The location of Cl was characterized by the Fourier synthesis of XRD patterns taken at room temperature after dehydration in vacuo at 623 K for 2 h (MAC Science, MXP3). The Graphic Fourier Program V1.12 and RIETAN94[19] were used for the Fourier synthesis and the pre-refinements of the patterns.

Differential thermal analysis (DTA) was performed to assess the stability of the starting zeolites. DTA curves were obtained with a Rigaku, Thermoflex8100 at a heating rate of 10 K/min under nitrogen flow.

Adsorption capacities of pure nitrogen and oxygen were obtained using a commercial volumetric apparatus (Belsorp 28SA, Bel Japan Inc.). Isotherms were measured at 298 K after dehydration in vacuo at 623 K for 2 h.

Results and Discussion

Amount of Occluded LiCl and Crystallinities. The results obtained for *ir*-LiCl/LiLSX are shown in Table 1. A control experiment conducted without a heat-treatment (Run 1) shows that the washing with dilute LiOH solution (pH = 11) was just enough to wash away unreacted LiCl, and to prevent hydrolysis. The Li/Al ratios of heat-treated zeolites (Runs 2–4) are above 1.00, showing that the LiCl was irreversibly occluded in the zeolite. The amount of occluded LiCl increased with the heat-treatment temperature. The Li/Al ratio of the sample heated at 898 K (Run 4) was 1.08, which approximately corresponds to one LiCl per sodalite cage. The XRD patterns of *ir*-LiCl/LiLSX (Fig. 2) are similar to those of LiLSX, and show no impurity peaks. The crystallinities of zeolites were also estimated from the XRD patterns. The crystallinity decreased with increasing heat-treatment temperature, as shown in Table 1. This reduction in crystallinity is believed to be due to the damage induced by the reaction between zeolite and LiCl.

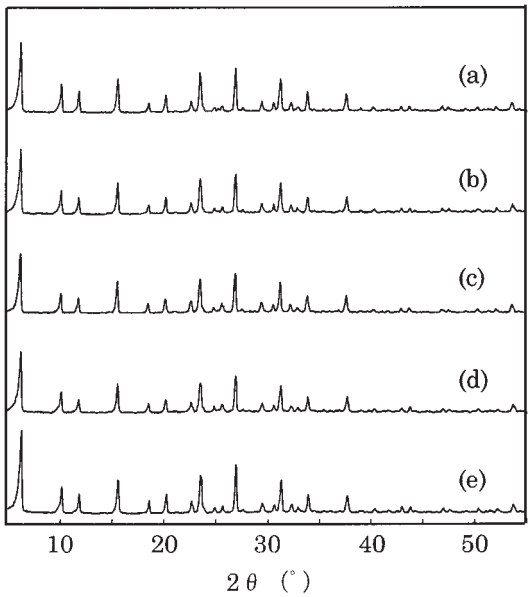

Fig. 2. XRD diffraction patterns of hydrated *ir*-LiCl/LiLSX. (a) Run 1, (b) Run 2, (c) Run 3, (d) Run 4, (e) Run 5.

Next, the starting zeolite was changed to NaLSX (Run 5). NaLSX slurried with a solution of LiCl was evaporated and heated at 898 K for 3 h, followed by lithium exchange. *ir*-LiCl/LiLSX prepared from NaLSX has almost the same amount of occluded LiCl as that prepared from LiLSX (Run 4), as well as high crystallinity (Table 1 and Fig. 2). The difference in the crystallinity between NaLSX and LiLSX as the

Table 1. Preparation Conditions and Experimental Results of *ir*-LiCl/LiLSX

Run	Preparation conditions		Experimental results		
	Starting zeolite	Condition of heat treatment	Li/Al[a)]	Relative crystallinity[b)]	Impurity[c)]
1	LiLSX	without heat treatment	1.00	—	—
2	LiLSX	863 K × 3 h	1.05	90%	none
3	LiLSX	873 K × 3 h	1.07	87%	none
4	LiLSX	898 K × 3 h	1.08	76%	none
5	NaLSX	898 K × 3 h	1.07	101%	none

a) Determined by inductively coupled plasma–atomic emission spectroscope. b) Estimated by XRD, compared with LiLSX heated at 863 K for 3 h. c) Ascertained by XRD.

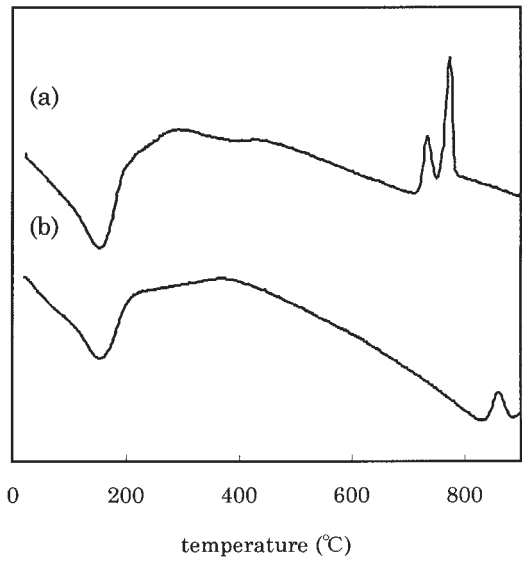

Fig. 3. DTA curves of (a) LiLSX and (b) NaLSX.

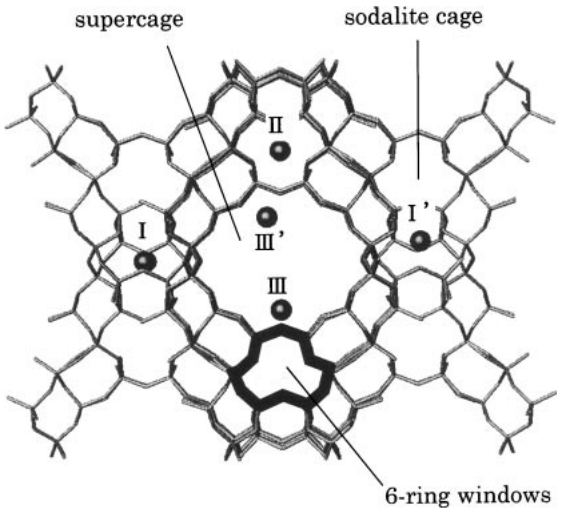

Fig. 4. Schematic diagram of LSX structure viewed from ⟨110⟩. I, I′, II, III, and III′ represent cation sites. (This drawing produced with ATOMS, by Shape Software.)

starting zeolites is thought to be due to the stability of the zeolites, themselves. The thermal stability was measured using DTA.

DTA curves of NaLSX and LiLSX are shown in Fig. 3. The exothermic temperature caused by the collapse of NaLSX was higher than that of LiLSX. This shows that NaLSX has a higher thermal stability than LiLSX. As described below, Cl anions are located in sodalite cages. Thus, the irreversible reaction between zeolite and LiCl presumably occurs by a movement of Cl anions from supercages to sodalite cages through the 6-ring windows (see Fig. 4). The diameter of the Cl anion (3.6 Å) is larger than the free diameter of negatively-charged 6-ring windows (2.2 Å).[3] The reaction is thought to induce stress on the zeolite skeletal structure. The angles of the T–O–T bond (T denotes Si or Al) in LiLSX are reported to be distorted compared with those in NaX.[20] The distortion of the skeletal structure, which is probably related to the thermal stability, would be difficult to withstand with a collapse of the structure accompanied by the movement of Cl anions from the supercages to the sodalite cages. Thus, *ir*-LiCl/LiLSX prepared from LiLSX has a lower crystallinity.

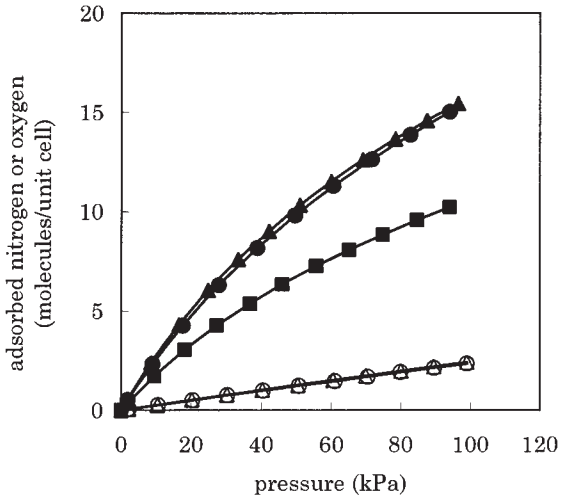

Fig. 5. Adsorption isotherms of nitrogen on *ir*-LiCl/LiLSX (●), LiLSX (▲), *re*-LiCl/LiLSX (■) and oxygen on *ir*-LiCl/LiLSX (○) and LiLSX (△) at 298 K.

Adsorption Properties of Nitrogen and Oxygen. Adsorption isotherms of pure nitrogen on high-crystallinity *ir*-LiCl/LiLSX with Li/Al = 1.07 (Run 5), *re*-LiCl/LiLSX with Li/Al = 1.08 and LiLSX at 298 K are shown in Fig. 5. The nitrogen isotherm of *ir*-LiCl/LiLSX matches that of LiLSX over the whole pressure range. Since there are fewer adsorbed molecules than main adsorption sites (32 Li cations at site III$^{(\prime)}$, as mentioned below), the results suggest that the numbers and states of the main adsorption sites are almost the same for *ir*-LiCl/LiLSX and LiLSX. Li cations occluded over the Al content would not affect the adsorption properties of nitrogen at room temperature.

On the other hand, the amount of adsorbed nitrogen on *re*-LiCl/LiLSX, which has approximately the same composition as *ir*-LiCl/LiLSX (Run 5), is less than that on LiLSX. *ir*-LiCl/LiLSX and *re*-LiCl/LiLSX differ with respect to the locations of the Li and Cl anions. Presumably, Cl anions in *re*-LiCl/LiLSX are coordinated with certain Li cations, and are located in the supercage. This suggests that the presence of Cl anions in the supercage decreases the number of nitrogen adsorption sites, i.e., Li cations at site III$^{(\prime)}$.

Oxygen adsorption isotherms of *ir*-LiCl/LiLSX (Run 5) and LiLSX are also shown in Fig. 5. The two isotherms virtually coincide, confirming that Li cations occluded over the Al content have no effect on the oxygen adsorption behavior at room temperature. *ir*-LiCl/LiLSX would perform as well as LiLSX as an adsorbent for oxygen pressure swing adsorption.

Location of Cl in Dehydrated *ir*-LiCl/LiLSX. An XRD Fourier synthesis of dehydrated *ir*-LiCl/LiLSX (Run 5) was performed to confirm the location of Cl anions in the zeolite structure. Figure 6 shows the observed profiles, the pre-refined profiles with the skeletal atoms of zeolites (Fd-3) by Rietveld analysis and their differential profiles for *ir*-LiCl/LiLSX and LiLSX. Figure 7 is a Fourier map at $z/c = 0.125$, calculated from the observed profiles. The Fourier map of *ir*-LiCl/LiLSX

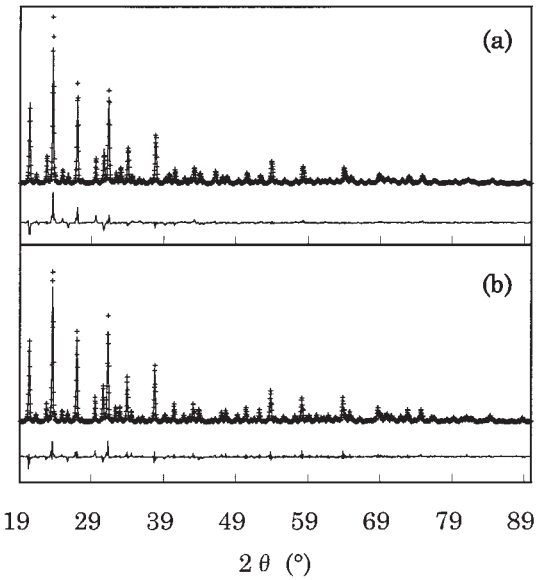

Fig. 6. XRD diffraction patterns of dehydrated (a) *ir*-LiCl/LiLSX and (b) LiLSX. Shown are observed patterns (+), pre-refined patterns (line), together with difference plots. R_{wp}, R_p, and s values of Rietveld analysis are 12.94, 10.04, and 3.99 in *ir*-LiCl/LiLSX, 12.76, 9.94, and 3.76 in LiLSX.

has a relatively high electron density region in the sodalite cage, at $x/a = y/b = z/c = 0.125$. It can safely be said that the electron density region is composed of Cl anions, because LiLSX has no high electron density regions in its sodalite cages. The location of the Cl anion is consistent with other Cl-occluded zeolite, which has a sodalite cage, such as NaCl-occluded sodalite[7,8] and NaCl-occluded CaY.[3]

Locations of Li in Dehydrated *ir*-LiCl/LiLSX. LSX has five different cation sites: I, I′, II, III, and III′, as shown in Fig. 4. Sites III and III′ are slightly different location-wise, but it was suggested that they are energetically equivalent.[21] So sites III and III′ are summarized in site III$^{(\prime)}$. The maximum number of cations that can be accommodated at sites I, I′, II, and III$^{(\prime)}$ per unit cell, taking into account cation–cation distances for site III$^{(\prime)}$, are 16, 32, 32, and 48, respectively.

LiLSX has 96 Li cations per unit cell, and it has been confirmed by neutron diffraction that dehydrated LiLSX has 32 Li cations per unit cell at each of the following sites: I′, II, and III$^{(\prime)}$,[20] as shown in Table 2. Sites I′ and II are fully occupied; site III$^{(\prime)}$ is partially occupied, and site I contains no Li cations.

On the other hand, *ir*-LiCl/LiLSX has up to 104 Li cations and up to 8 Cl anions per unit cell because one sodalite cage can accommodate up to one LiCl. Next, we consider the possible locations for Li cations.

First, the number of Li being located at site III$^{(\prime)}$ is considered. As mentioned above, the nitrogen adsorption properties of *ir*-LiCl/LiLSX at room temperature are similar to those of LiLSX. On the other hand, it is generally accepted that LiLSX mainly adsorbs nitrogen on Li cations at site III$^{(\prime)}$.[21–25] It is thus suggested that, like LiLSX, dehydrated *ir*-LiCl/LiLSX has 32 Li cations at site III$^{(\prime)}$ per unit cell.

Next, sites I′ and II are considered. XRD Fourier synthesis

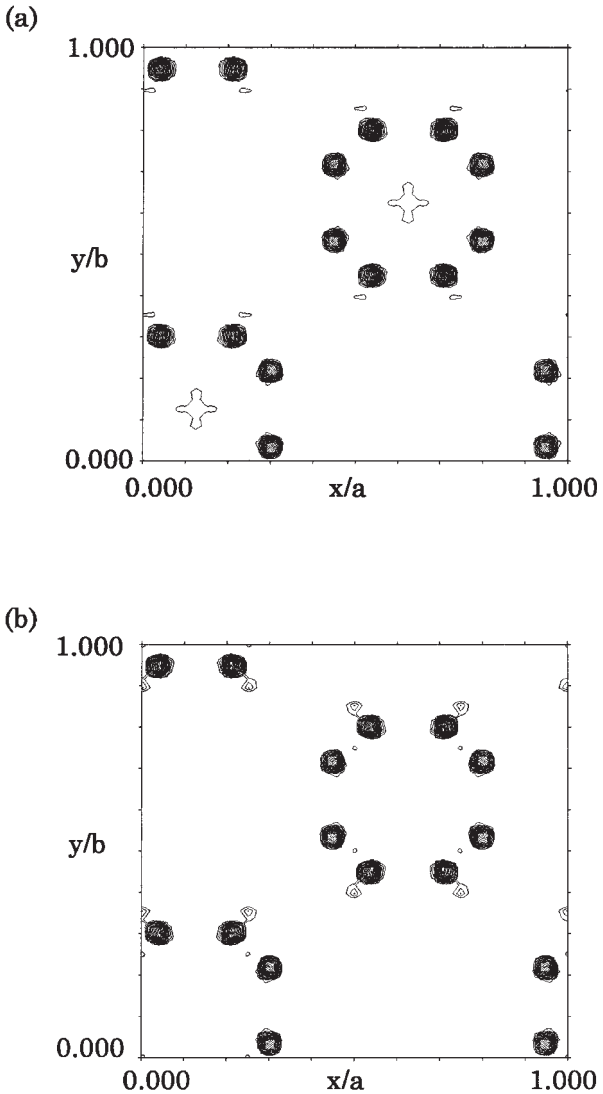

Fig. 7. Fourier synthesis map ($z/c = 0.125$) of (a) dehydrated *ir*-LiCl/LiLSX and (b) dehydrated LiLSX from the observed pattern after the pre-optimization of zeolite skeleton.

Table 2. Possible Locations of Li Cations and Cl Anions in Dehydrated *ir*-LiCl/LiLSX

Site	Maximum number per unit cell	*ir*-LiCl/LiLSX[a)]	cf) LiLSX[b)]
III$^{(\prime)}$	48[c)]	32 Li	32 Li
II	32	32 Li	32 Li
I′	32	32 Li	32 Li
I	16	8 Li	—
U[d)]	8	8 Cl	—

a) Possible locations. b) Analyzed locations by neutron powder diffraction (Ref. 20). c) The maximum number of cations at site III$^{(\prime)}$ taking account of cation–cation distances. d) Site U is at the center of the sodalite cage.

revealed that chloride anions in *ir*-LiCl/LiLSX are located in sodalite cages. There are numerous reports that four monovalent cations in halogen-salt occluded zeolites are tetrahedrally

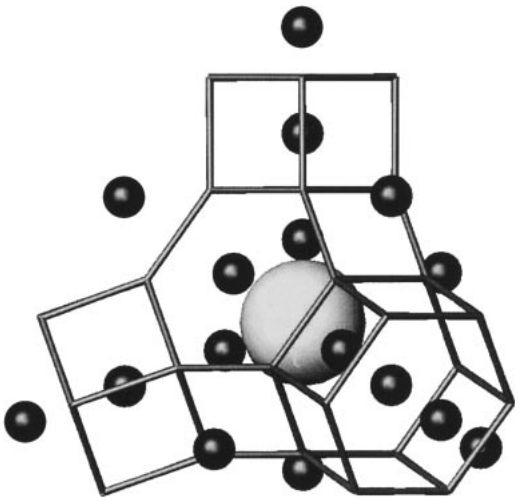

Fig. 8. Possible Li locations in dehydrated *ir*-LiCl/LiLSX, drawn in sodalite cage with double 6-rings. Light gray ball shows a Cl anion and dark gray balls show Li cations. (This drawing produced with ATOMS, by Shape Software.)

coordinated to a halogen anion in sodalite cages, e.g., four Li cations tetrahedrally coordinated to a Cl anion in LiCl-occluded sodalite[11] and four Na cations tetrahedrally coordinated to a Cl anion in NaCl-occluded NaY.[13] Thus, *ir*-LiCl/LiLSX would have four Li cations tetrahedrally coordinated to a Cl anion, forming one Li_4Cl^{3+} cluster per sodalite cage (totaling 32 Li and 8 Cl per unit cell). Li cations of the Li_4Cl^{3+} cluster would be located at site I′, shifted towards Cl anions from their normal position at site I′. Furthermore, states of Li at site II would not be affected by a Li_4Cl^{3+} cluster in a sodalite cage. Thus, 32 Li cations are presumably located at site II, as in the case with LiLSX.

The residuals are 8 Li cations. It is well accepted that the adjacent sites I and I′ cannot simultaneously be occupied.[26] However, in the case of salt-occluded FAU with a high aluminum content, adjacent sites I and I′ may be occupied simultaneously because cations at site I′ would shift toward the anion and the double 6-ring windows are highly charged. *ir*-LiCl/LiLSX may have 8 Li at site I per unit cell. Table 2 gives the possible locations of Li cations in *ir*-LiCl/LiLSX, and Fig. 8 schematizes the possible locations in *ir*-LiCl/LiLSX drawn in a sodalite cage with double 6-rings.

Conclusions

ir-LiCl/LiLSX was prepared from LiLSX or NaLSX by varying the heat-treatment temperature with LiCl. As the heat-treatment temperature of the mixture of LiLSX and LiCl increased, the amount of occluded LiCl increased, but the crystallinity of the resultant *ir*-LiCl/LiLSX was lowered. *ir*-LiCl/LiLSX prepared from a heat treatment of NaLSX with LiCl, followed by lithium exchange, exhibited high crystallinity. The difference in the crystallinity induced by differences in the preparation method is explained as being related to the difference in the distortion of the skeleton structure of the zeolites.

The irreversible occlusion of LiCl in the LiLSX has no influence on the adsorption properties of nitrogen or oxygen at room temperature, despite the increase in the number of Li cations per unit cell. Chloride anions in *ir*-LiCl/LiLSX were found to be located in the sodalite cages. The possible locations of Li cations are deduced from the adsorption properties of nitrogen and existing data on salt-occluded zeolites.

We would like to thank Prof. K. Tsutsumi of Toyohashi University of Technology for discussions and suggestions regarding this work.

References

1 R. M. Barrer and W. M. Meier, *Trans. Faraday Soc.*, **54**, 299 (1958).

2 J. A. Rabo, M. L. Poutsma, and G. W. Skeels, "Proceedings of the 5th International Congress on Catalysis," North Holland Publishing, Amsterdam (1973), p. 1353.

3 J. A. Rabo, "Zeolite Chemistry and Catalysis," ACS Monograph 171, American Chemical Society (1976), Chapter 5.

4 R. M. Barrer, "Hydrothermal Chemistry of Zeolites," Academic Press (1982), Chapter 7.

5 A. Seidel, U. Tracht, and B. Boddenberg, *J. Phys. Chem.*, **100**, 15917 (1996).

6 J. Godber and G. A. Ozin, *J. Phys. Chem.*, **92**, 4980 (1988).

7 L. Pauling, *Z. Kristallogr.*, **74**, 213 (1930).

8 R. K. McMullan, S. Ghose, N. Haga, and V. Schomaker, *Acta Crystallogr., Sect. B*, **B52**, 616 (1996).

9 H. Trill, H. Eckert, and V. I. Srdanov, *J. Am. Chem. Soc.*, **124**, 8361 (2002).

10 V. J. Loens and H. Schulz, *Acta Crystallogr.*, **23**, 434 (1967).

11 M. T. Weller and G. Wong, *Solid State Ionics*, **32/33**, 430 (1989).

12 U. Tracht, A. Siedel, and B. Boddenberg, *Stud. Surf. Sci. Catal.*, **105**, 525 (1997).

13 A. Seidel, B. Schimiczel, U. Tracht, and B. Boddenberg, *Solid State Nucl. Magn. Reson.*, **12**, 53 (1998).

14 S. Macura and D. Vucelic, "Proceedings the 5th International Conference on Zeolites," Imperial College of Science and Technology (1980), p. 327.

15 M. A. Lewis, D. F. Fischer, and L. J. Smith, *J. Am. Ceram. Soc.*, **76**, 2826 (1993).

16 M. F. Simpson and T. J. Battisti, *Ind. Eng. Chem. Res.*, **38**, 2469 (1999).

17 S. U. Rege and R. T. Yang, *Ind. Eng. Chem. Res.*, **36**, 5358 (1997).

18 G. H. Kuhl, *Zeolites*, **7**, 451 (1987).

19 F. Izumi, "The Rietveld Method," ed by R. A. Young, Oxford University Press, Oxford (1993), pp. 236–253.

20 J. Plevert, F. D. Renzo, F. Fajula, and G. Chiari, *J. Phys. Chem. B*, **101**, 10340 (1997).

21 S. R. Jale, M. Bulow, F. R. Fitch, N. Perelman, and D. Shen, *J. Phys. Chem. B*, **104**, 5272 (2000).

22 M. Feuerstein, G. Engelhardt, P. L. McDaniel, J. E. MacDougall, and T. R. Gaffney, *Microporous Mesoporous Mater.*, **26**, 27 (1998).

23 M. Feuerstein and R. F. Lobo, *Chem. Commun.*, **1998**, 1647.

24 S. Yoshida, N. Ogawa, K. Kamioka, S. Hirano, and T. Mori, *Adsorption*, **5**, 57 (1999).

25 N. D. Hutson, S. C. Zajic, and R. T. Yang, *Ind. Eng. Chem. Res.*, **39**, 1775 (2000).

26 E. Dempsey, *J. Phys. Chem.*, **73**, 3660 (1969).